

Optimization of Multi-Layer Metal Neural Probe Design

Angela Tooker, Vanessa Tolosa, Kedar G. Shah, Heeral Sheth, Sarah Felix, Terri Delima,
Satinderpall Pannu

Abstract— We present here a microfabrication process for multi-layer metal, multi-site, polymer-based neural probes. The process has been used to generate 1-, 2-, and 4-layer trace metal neural probes with highly uniform and reproducible electrode characteristics. Typically, increasing the number of metal layers is assumed to both reduce the width of the neural probes and minimize the injury and glial scarring caused at the implantation site. We show, however, that increasing the number of trace metal layers does not always result in the minimal probe cross-sectional area. A thorough design analysis reveals that the electrode size, along with other design parameters, have interacting effects on the probe cross-sectional area. Moreover, increasing the trace metal layers in the neural probes also increases the design and fabrication cost/time, as well as the likelihood of probe failure. Consequently, all of these factors must be considered when designing a multi-site, neural probe with the objective of minimizing tissue damage.

I. INTRODUCTION

There is an ever-present need for reliable, biocompatible interfaces for chronic recording and stimulation of neural tissue. This capability is required for identifying and understanding the underlying mechanisms of the complex nervous system and developing neural prosthetics to treat debilitating, chronic, neurological disorders, such as deafness, blindness, spinal cord injury, depression, and several brain-related diseases (i.e. Parkinson's disease and epilepsy). Many of the basic neuroscience questions remain unresolved due to our lack of ability to simultaneously interface with a large population of neurons. Implantable, multi-site, neural probes are ideally suited for simultaneously recording and stimulating large numbers of neurons. Applications of implantable, multi-site, neural interfaces (e.g. cochlear and retinal implants) have proven to be successful to date; however, further technological improvement is still required.

A variety of different microfabricated, multi-site, polymer-based neural probes are currently in use for recording and stimulation of neural tissue [1-6]. The neural probes consist of multiple, discrete electrodes that are connected, via metal traces, to output leads and/or other signal processing circuitry. Neuronal stimulation and

recording is conducted at these electrode sites. Flexible polymers, such as polyimide or parylene, are eminently suitable as the backbone for these neural probes as their mechanical properties are closely matched to that of neural tissue. Thus, the polymer-based neural probes will impart less strain on the neural tissue, compared to stiffer materials (e.g. silicon or metal) resulting in less injury and glial scarring at the implantation site [7]. In addition, polyimide and parylene are both biocompatible materials; thus, they are both suitable for chronic, long-term implantation [8].

Although the use of the flexible polymer minimizes the injury and glial scarring caused by the implantation of the neural probe, it does not eliminate it. The amount of injury and scarring can be further reduced by minimizing the size (i.e. cross-sectional area) of the implanted neural probe. Unfortunately, typical efforts to minimize the width of the implanted probe limit the number of stimulation and recording sites (electrodes). In order to effectively decrease the width of the probe, while maintaining the electrode count, additional trace metal routing layers are required. These additional metal layers will necessitate adding additional polymer insulating layers, thereby increasing the total thickness of the probe by 1 – 2 μm per layer. Generally, the width of the polymer-based neural probes is 20 – 30 times the thickness. Thus, if a significant decrease in probe width can be achieved, for a given number of electrodes, with only a marginal increase in probe thickness, the resulting size (cross-sectional area) of the neural probe can be minimized, causing less injury and scarring.

There are several examples of microfabricated, multi-site, polyimide neural probes with one layer of trace metal [1-2]. In addition, some work has been done using two layers of trace metal [3-6]. We present here a microfabrication process for a multi-site, polymer-based, neural probe with four layers of trace metal. In addition, we explore the optimization of neural probe designs considering electrode size and the number of metal layers and the resulting neural probe cross-sectional areas.

II. NEURAL PROBE DESIGN AND FABRICATION

Three different multi-site, neural probes were designed: 1-layer metal, 2-layer metal, and 4-layer metal. Each neural probe has 16 electrodes (100 μm in diameter). The same design guidelines (e.g. trace metal width/spacing, electrode spacing, and metal-to-edge distance) were used in all designs. For the 2-layer and 4-layer metal probes, the layers of trace metal are connected using interconnection vias. For simplicity, the neural probes are designed such that the interconnection vias are outside of the active exposed

* Research supported by National Institute of Deafness and Other Communication Diseases.

A. C. Tooker is with Lawrence Livermore National Laboratory, Livermore, CA 94550 USA (phone: 925-422-2326; fax: 925-422-2373; e-mail: tooker1@llnl.gov).

V. Tolosa, K.G. Shah, H. Sheth, S. Felix, T. Delima, and S. Pannu are with Lawrence Livermore National Laboratory, Center for Micro- and Nano-Technology, Livermore, CA 94550 USA (e-mail: tolosa1@llnl.gov, shah22@llnl.gov, sheth2@llnl.gov, felix5@llnl.gov, delima1@llnl.gov, pannu1@llnl.gov).

electrodes; also, the trace metal is not routed directly underneath the active exposed electrodes.

The general fabrication process for the 2-layer metal, multi-site, polymer neural probes, shown in Fig. 1, utilizes standard MEMS fabrication techniques. The processing steps are summarized below:

1. Polyimide 1 Deposition (5 μm)
2. Deposition and patterning of Trace Metal 1 (Ti/Au/Ti)
3. Polyimide 2 Deposition (2 μm)
4. Interconnection Via etching (O_2 plasma)
5. Deposition and patterning of Trace Metal 2 (Ti/Au/Ti)
6. Deposition and patterning of Electrode Metal (Ir)
7. Polyimide 3 Deposition (5 μm)
8. Electrode Via etching (O_2 plasma)
9. Device Outline etching (O_2 plasma)

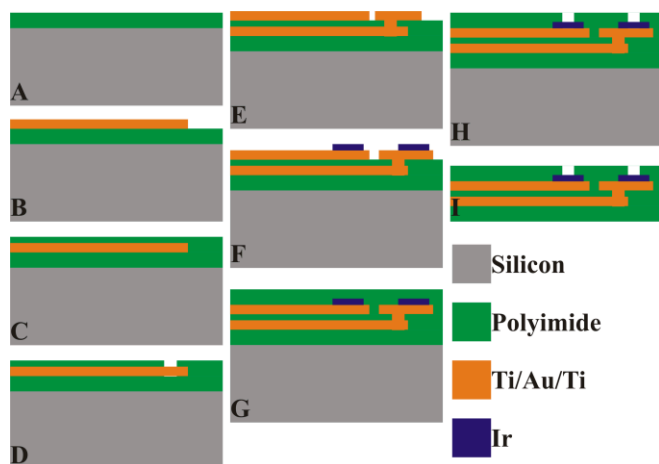


Figure 1. Cross-sectional view of the general fabrication process for polyimide neural probes with 2 layers of trace metal. (Images are not drawn to scale.)

The 1-layer and 4-layer metal, multi-site, polymer neural probes undergo similar processing steps. For the 1-layer metal neural probes, processing steps 3, 4, and 5 are eliminated (Fig. 2). For the 4-layer metal neural probes, processing steps 3, 4, and 5 are repeated a total of three times to create the four layers of trace metal (Fig. 3). We have demonstrated this process using polyimide. The same fabrication process can be used with other polymers, such as parylene and silicones.



Figure 2. Cross-sectional view of the polyimide neural probe with 1 layer of trace metal. (Images are not drawn to scale.)

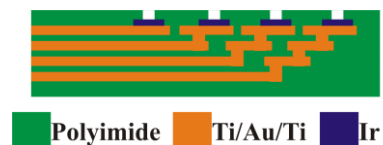


Figure 3. Cross-sectional view of the polyimide neural probe with 4 layers of trace metal. (Images are not drawn to scale.)

Photographs of the 1-layer, 2-layer, and 4-layer metal, multi-site, polymer neural probes with 100 μm diameter electrodes are shown in Figs. 4-6. (The interference patterns visible in Figs. 4-6 result from the non-uniformity of the polyimide laying down on the glass slide.) The 16-electrode, 1-layer metal neural probe (Fig. 4) has no interconnection vias. The 16-electrode, 2-layer metal neural probe (Fig. 5) has 8 interconnection vias total allowing half of the electrodes to be routed on each trace metal layer. The 16-electrode, 4-layer metal probe (Fig. 6) has 4 electrodes routed on each trace metal layer. The electrodes routed on Trace Metal 1, 2, and 3 have 3, 2, and 1 interconnection vias, respectively.

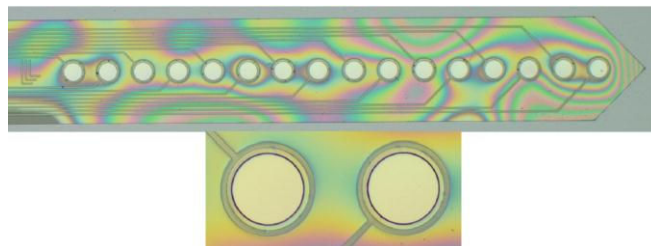


Figure 4. A 16-electrode, 1-layer metal, neural probe (top). Since only 1 layer of trace metal is used, there are no interconnection vias. An enlarged view of the 100 μm diameter electrodes is shown at the bottom.

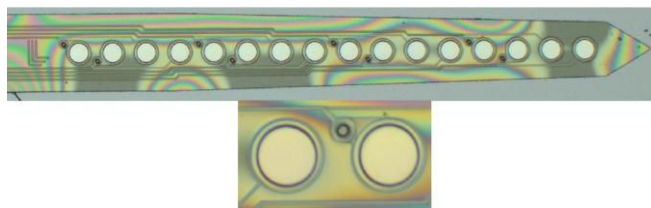


Figure 5. A 16-electrode, 2-layer metal, neural probe (top). There are a total of 8 interconnection vias (one for every other electrode). An enlarged view of the 100 μm diameter electrodes is shown at the bottom; the interconnection via is visible next to the bottom-right electrode.

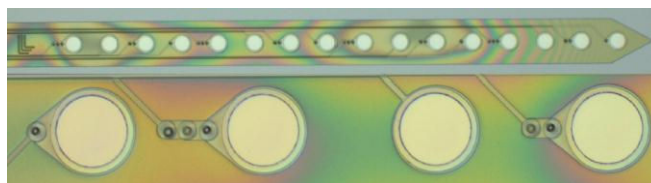


Figure 6. A 16-electrode, 4-layer metal, neural probe (top). An enlarged view of the 100 μm diameter electrodes with their interconnection vias is also shown (bottom). In the bottom image, the electrodes are routed on Trace Metal 3, 1, 4, and 2, from left-to-right, respectively.

III. ELECTRODE CHARACTERIZATION

The iridium activation was performed using biphasic potential pulsing in phosphate-buffered saline to form an activated iridium oxide film (AIROF). Individual iridium electrodes were characterized to determine charge storage capacity (CSC) and impedance both before and after activation. Cyclic voltammetry (CV) and electrochemical impedance measurements were made with a Princeton Applied Research (PAR) potentiostat using vendor-supplied software. All measurements were made in a three-electrode cell using a Pt counter electrode, an Ag/AgCl reference electrode, and phosphate-buffered saline (pH 7.4) as the

electrolyte. A summary of the CSC and impedance data for the different multi-site, neural probes, before and after activation is shown in Table I. It is expected for a given electrode design, the electrochemical properties should remain constant, regardless of the number of trace metal layers used. The introduction of additional trace metal layers necessitates the use of interconnection vias; however, the impedance from the additional trace metal should be negligible compared to the electrode's impedance. As the data shows, regardless of the number of trace metal layers used, there is no significant difference in electrode characteristics. The minor differences observed in the electrochemical properties of the electrodes can likely be attributed to process variations occurring during the different neural probe fabrications.

TABLE I. NEURAL PROBE ELECTRODE CSC AND IMPEDANCE DATA

Neural Probe	Iridium		AIROF	
	CSC Average (Std. Dev.)	Impedance ($f = 1$ kHz)	CSC Average (Std. Dev.)	Impedance ($f = 1$ kHz)
1-Layer Metal ^a (n = 32)	2.93 mC/cm ² (0.50)	~13 k Ω	21.15 mC/cm ² (1.10)	~3 k Ω
2-Layer Metal ^a (n = 16)	2.12 mC/cm ² (0.10)	~10 k Ω	19.58 mC/cm ² (0.22)	~4 k Ω
4-Layer Metal ^a (n = 32)	2.63 mC/cm ² (0.41)	~10 k Ω	21.18 mC/cm ² (0.18)	~4 k Ω

a. All data is for 100 μ m diameter electrodes.

IV. NEURAL PROBE DESIGN OPTIMIZATION

As we have demonstrated, multi-site, multi-layer metal, neural probes can be fabricated with uniform and reproducible electrode characteristics, regardless of the number of metal layers used. This has not been demonstrated before. The primary objective is to reduce the injury and glial scarring that can occur at the implantation site by minimizing the neural probe cross-sectional area, without decreasing the number of recording/stimulating sites. The width of the probe can be reduced by introducing additional trace metal layers. Each additional trace metal layer, however, increases the thickness of the probe. We used our design guidelines to determine the relationship between electrode size, number of metal layers, and neural probe cross-sectional area. (The cross-sectional area of the probe is calculated by multiplying the width of the probe by the height of the probe.) In the analysis, we assumed: 1) a 1-layer metal neural probe has a thickness of 10 μ m, 2) each additional metal layer increased the probe thickness by 2 μ m, and 3) for simplicity, trace metal is not routed directly underneath the active exposed electrodes. For the purposes of this analysis, the following design specifications were used: trace metal width = 6 μ m, trace metal spacing = 6 μ m, and polyimide edge-to-metal distance = 10 μ m. The calculations were all performed for a 16-electrode neural probe. Fig. 7 shows the relationship between the probe cross-sectional area and the electrode diameter for different numbers of trace metal layers. For a given number of trace metal layers, the relationship between the electrode diameter and the probe cross-sectional area is linear. However, for a

given electrode diameter, the relationship between the minimal probe cross-sectional area and the number of trace metal layers is more complicated. For small electrodes (< 80 μ m diameter), the minimal probe cross-sectional area is achieved with 4 layers of trace metal. For medium-sized electrodes (> 80 μ m and < 360 μ m diameter), the minimal probe cross-sectional area is achieved with 2 layers of trace metal. For large electrodes (> 360 μ m diameter), the minimal probe cross-sectional area is actually achieved with only 1 layer of trace metal. The specific electrode diameter values that serve as the boundaries between the small, medium, and large electrodes (in this case 80 μ m and 360 μ m) are dependent upon the design specifications used. If, for example, the polyimide edge-to-metal distance was increased to 25 μ m, the boundaries between the small, medium, and large electrodes would be 40 μ m and 330 μ m. The same general trends are still valid though, i.e. for electrode diameters < 40 μ m the minimal probe cross-sectional area is achieved with 4 layers of trace metal and for electrode diameters > 330 μ m the minimal probe cross-sectional area is achieved with 1 layer of trace metal. Although not specifically addressed here, if the resistance of the trace metal is a key parameter, the use of additional trace metal layers allows the trace widths to increase without a concurrent increase in probe width.

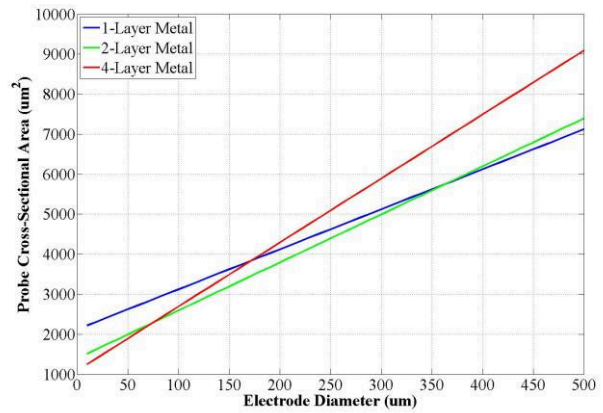


Figure 7. The minimal probe cross-sectional area is a function of both the electrode diameter and the number of trace metal layers. As this graph shows, simply increasing the number of trace metal layers does not always result in the minimal probe cross-sectional area.

Although not reflected in this analysis is the additional cost and time in neural probe design for adding additional trace metal layers. More importantly, however, the fabrication cost/time and the likelihood of failure are both increased. With each additional trace metal layer that is added, more interconnection vias are required. Unfortunately, the interconnection vias introduce a failure point for these polyimide neural probes, typically due to cracking of the metal at the base of the vias. Thus, minimizing the number of interconnection vias is desirable. While for some electrode sizes (e.g. 10 μ m), there is a significant decrease in probe cross-sectional area for both 2- and 4-layers of trace metal, thereby justifying the increased design/fabrication time and costs, for other electrode sizes the advantage is less obvious (Table II). For the 70 μ m diameter electrode, there is an obvious reduction in probe

cross-sectional area for 2 layers of trace metal, compared to 1 layer of trace metal. While there is a further reduction in probe cross-sectional area for 4 layers of trace metal, it is not obvious that the additional $24 \mu\text{m}^2$ reduction ($\sim 1\%$) justifies the additional fabrication cost/time and the increased cost of probe failure. Similarly, for the $300 \mu\text{m}$ diameter electrode, using 4 layers of trace metal will dramatically increase the probe cross-sectional area, compared to either 1- or 2-layers of metal. Again, however, it is not obvious if the 2.5% reduction gained by increasing from 1 to 2 layers of trace metal imparts a significant advantage.

TABLE II. CHANGE IN PROBE CROSS-SECTIONAL AREA FOR DIFFERENT METAL LAYERS

Electrode Diameter ^a	Neural Probe Cross-Sectional Area (% Area Change ^b)		
	1-Layer Metal	2-Layer Metal	4-Layer Metal
10 μm	2220 μm^2	1512 μm^2 (-31.9%)	1248 μm^2 (-43.8%)
70 μm	2820 μm^2	2232 μm^2 (-20.9%)	2208 μm^2 (-21.7%)
300 μm	5120 μm^2	4992 μm^2 (-2.5%)	5888 μm^2 (+15.0%)

a: Assumes a 16-electrode neural probe.

b. All % area changes use the 1-Layer Metal as a reference.

In addition to the increases in both the fabrication cost/time and the likelihood of probe failure, adding more and more trace metal layers will increase the mechanical stiffness of the polymer-based neural probe. According to beam theory, mechanical stiffness is proportional to the thickness cubed. Our qualitative observations have shown that thicker probes are stiffer; the different neural probes are currently undergoing testing to quantitatively determine the mechanical stiffness caused by the increased probe thickness. The possibility of inducing additional injury or scarring increases with the mechanical stiffness of the probe, thereby possibly negating the advantages gained with the reduction in cross-sectional area. Specific applications, however, will dictate the allowable probe stiffness, and will impart further design constraints.

This analysis also highlights the distinct advantage of the dual-side, multi-site, neural probes [4-6, 9]. Table III shows the reduction in cross-sectional area obtained for a specified number of electrodes in a dual-sided neural probe, compared to a single-sided neural probe. For the design specifications used here, a dual-sided neural probe with the same number of individually-addressable electrodes has a 16.7% reduction in probe cross-sectional area, compared to the single-sided neural probe.

V. CONCLUSION

We have demonstrated a fabrication process for multi-site, multi-layer metal, polymer neural probes with uniform and reproducible electrode characteristics, regardless of the number of metal layers used. The relationship between the electrode size and the probe cross-sectional area is linear; however, increasing the number of trace metal layers does not always result in the minimal probe cross-sectional area, for a given number of electrodes. Therefore, if the objective is to reduce the injury and glial scarring at the implantation

site by reducing the neural probe size, it is important to consider both the electrode diameter and number of trace metal layers when designing the probe. Further, the additional costs incurred in design and fabrication cost/time, as well as the increased likelihood of probe failure, may not be justified for only marginal reductions in probe cross-sectional area. This analysis also points to the significant advantage of dual-sided neural probes for increasing the number of individually-addressable electrodes without increasing the probe cross-sectional area.

TABLE III. COMPARISON OF THE PROBE CROSS-SECTIONAL AREAS FOR SINGLE-SIDED AND DUAL-SIDED NEURAL PROBES

Number of Electrodes ^a	Probe Cross-Sectional Area ^b	
	Single-Sided Neural Probe	Dual-Sided Neural Probe
16	2592 μm^2	2160 μm^2
24	3168 μm^2	2640 μm^2
32	3744 μm^2	3120 μm^2
48	4896 μm^2	4080 μm^2
64	6048 μm^2	5040 μm^2

a. For the dual-sided neural probe, half of the electrodes are on top and half are on the bottom; the total number of electrodes is as shown. All electrodes are individually-addressable.

b. Assumes a 100 μm diameter electrode.

ACKNOWLEDGMENT

This work has been funded by the National Institute of Deafness and Other Communication Diseases. This work performed under the auspices of the U.S. Department of Energy by Lawrence Livermore National Laboratory under Contract DE-AC52-07NA27344. LLNL-ABS-538831.

REFERENCES

- [1] S. Lee, J. Jung, Y. Chae, J.-K. Suh, and J. Kang, "Fabrication and characterization of implantable flexible nerve cuff electrodes with Pt., Ir, and IrO_x films deposited by RF sputtering," *J. Micromech. Microeng.*, vol. 20, no. 3, March 2010.
- [2] B. Rubehn, C. Bosman, R. Oostenveld, P. Fries, and T. Stieglitz, "A MEMS-based flexible multi-channel ECoG-electrode array," *J. Neural Eng.*, vol. 6, no. 3, June 2009.
- [3] A. Mercanzini, K. Cheung, D. Buhl, M. Boers, A. Maillard, P. Colin, J.-C. Bensadoun, A. Bertsch, and P. Renaud, "Demonstration of cortical recording using novel flexible polymer neural probes," *Sens. Actuators A*, vol. 143, pp. 90-96, 2008.
- [4] J. Seymour, N. Langhals, D. Anderson, and D. Kipke, "Novel multi-side, microelectrode arrays for implantable neural applications," *Biomed. Microdevices*, vol. 13, pp. 441-451, February 2011.
- [5] T. Doerge, S. Kammer, M. Hanauer, A. Sossalla, S. Steltenkamp, "Novel method for a flexible double sided microelectrode fabrication process," *Bioengineered and Bioinspired Systems IV Book Series: Proc. Of SPIE*, vol. 7365, 2009.
- [6] T. Stieglitz, "Flexible biomedical microdevices with double-sided electrode arrangements for neural applications," *Sens. Actuators A*, vol. 90, pp. 203-211, 2001.
- [7] V. Polikov, P. Tresco, and W. Reichert, "Response of brain tissue to chronically implanted neural electrodes," *J. Neurosci. Meth.*, vol. 148, pp. 1-18, 2005.
- [8] Y. Sun, S. Lacour, R. Brooks, R. Rushton, J. Fawcett, and R. Cameron, "Assessment of the biocompatibility of photosensitive polyimide for implantable medical device use," *J. Biomed. Mat. Res. A*, vol. 90A, no. 3, pp. 648-655, September 2009.
- [9] A. Tooker, V. Tolosa, K.G. Shah, H. Sheth, S. Felix, T. Delima, and S. Pannu, "Polymer Neural Interface with Dual-Sided Electrodes for Neural Stimulation and Recording," in *Proc. 34th IEEE Eng. Med. Biol. Soc. Ann. Int. Conf. 2012*, to be published.